




Article

NO_x Storage on BaTi_{0.8}Cu_{0.2}O₃ Perovskite Catalysts: Addressing a Feasible Mechanism

Vicente Albaladejo-Fuentes ¹, María-Salvadora Sánchez-Adsuar ¹, James A. Anderson ²
and María-José Illán-Gómez ^{1,*}

¹ Carbon Materials and Environment Research Group, Department of Inorganic Chemistry, Faculty of Science, Universidad de Alicante San Vicente del Raspeig, 03690 Alicante, Spain; vicentealbaladejo@gmail.com (V.A.-F.); dori@ua.es (M.-S.S.-A.)

² Surface Chemistry and Catalysis Group, School of Engineering, University of Aberdeen, Aberdeen AB24 3UE, UK; j.anderson@abdn.ac.uk

* Correspondence: illan@ua.es

Abstract: The NO_x storage mechanism on BaTi_{0.8}Cu_{0.2}O₃ catalyst were studied using different techniques. The results obtained by XRD, ATR, TGA and XPS under NO_x storage–regeneration conditions revealed that BaO generated on the catalyst by decomposition of Ba₂TiO₄ plays a key role in the NO_x storage process. In situ DRIFTS experiments under NO/O₂ and NO/N₂ show that nitrites and nitrates are formed on the perovskite during the NO_x storage process. Thus, it seems that, as for model NSR catalysts, the NO_x storage on BaTi_{0.8}Cu_{0.2}O₃ catalyst takes place by both “nitrite” and “nitrate” routes, with the main pathway being highly dependent on the temperature and the time on stream: (i) at T < 350 °C, NO adsorption leads to nitrites formation on the catalyst and (ii) at T > 350 °C, the catalyst activity for NO oxidation promotes NO₂ generation and the nitrate formation.

Keywords: NO_x storage mechanism; in situ DRIFTS; nitrites; nitrates; barium-titanium perovskite



Citation: Albaladejo-Fuentes, V.; Sánchez-Adsuar, M.-S.; Anderson, J.A.; Illán-Gómez, M.-J. NO_x Storage on BaTi_{0.8}Cu_{0.2}O₃ Perovskite Catalysts: Addressing a Feasible Mechanism. *Nanomaterials* **2021**, *11*, 2133. <https://doi.org/10.3390/nano11082133>

Academic Editor: Karthik Shankar

Received: 14 July 2021

Accepted: 17 August 2021

Published: 21 August 2021

Publisher's Note: MDPI stays neutral with regard to jurisdictional claims in published maps and institutional affiliations.



Copyright: © 2021 by the authors. Licensee MDPI, Basel, Switzerland. This article is an open access article distributed under the terms and conditions of the Creative Commons Attribution (CC BY) license (<https://creativecommons.org/licenses/by/4.0/>).

1. Introduction

NO_x Storage and Reduction (NSR) is one of the proposed technologies for the effective abatement of NO_x from exhaust gas emitted by lean burn engines. A typical NSR catalyst is composed of a noble metal (mainly Pt and/or Rh) and an alkaline/alkaline earth oxide, both supported on high-surface aluminum oxide [1]. Based on the high chemisorption capacity of the alkaline/alkaline earth oxide, the NSR catalyst is able to store a high amount of NO_x during the short time of the lean conditions step (oxygen rich atmosphere). Periodically, a reducing agent is fed in the gas exhaust system (rich conditions), which induces the release and reduction of the previously stored NO_x and, as a result, the regeneration of the catalyst surface [2,3]. Thus, the NSR process involves several steps: (i) during the lean cycle, NO (main nitrogen oxide compound in gas exhaust conditions) to NO₂ oxidation followed by its storage in the form of nitrites/nitrates on the surface of the basic oxide component of the catalyst, while afterwards, (ii) during the rich cycle, reductant feed or generation causes NO_x release from the catalyst and their subsequent reduction to N₂ [4].

A wide number of reports dealing with the study of the NO_x storage and reduction mechanism on NSR model catalysts have been published [5–18]. According to the NO_x storage mechanism proposed by Fridell and co-workers [5], NO₂, coming from the oxidation of NO onto Pt active sites, is mainly adsorbed on BaO forming surface nitrates by a disproportionation reaction that involves the release of one molecule of NO for every three molecules of NO₂ adsorbed (1).



Recently, Broqvist et al. [6] suggested, supported by DFT calculations, that NO₂ adsorption on a BaO surface can take place either on oxygen surface sites or on Ba (II) sites

forming nitrates and nitrites, respectively. The generation of the nitrate–nitrite pairs involves a partial oxidation of the surface, and finally, only nitrates would be the unique ending species present on the surface. However, NO_x in exhaust gases is mainly present as a NO/O₂ mixture, which suggests that this route, which only considers NO₂ adsorption, might not be the main one for the NO_x storage mechanism. Recently, based on transient response experiments and operando FTIR studies, Lietti and co-workers [11] demonstrated the existence of the called “nitrite route” for NO_x storage in NO/O₂ atmosphere. These authors concluded that, firstly, at low temperature, nitrites can be formed on the BaO surface after the NO oxidation at Pt–BaO boundaries. At high temperature, this route will lead to subsequent nitrites to nitrates formation.

Using perovskite mixed oxides, Hodjati et al. [19] and Milt et al. [20] proposed that NO_x was adsorbed on BaSnO₃ and BaCoO₃ perovskites forming barium nitrates, respectively. These nitrates could decompose at high temperature in an oxidizing atmosphere, allowing the regeneration of the perovskite; however, the high temperature for nitrate desorption induced the segregation of a low fraction of B cation oxide from the perovskite lattice. Abrahamsson et al. [21] concluded (from DFT results) that NO₂ was more strongly adsorbed than NO on ATiO₃ perovskite surfaces, but NO and NO₂ co-adsorption enhanced the stability of the ad-species due to nitrite-nitrate pair formation. Additionally, López-Suárez et al. [22], using SrTi_{1-x}Cu_xO₃ perovskites, observed that NO_x chemisorption could take place by adsorption of NO as nitrites and/or oxidation of NO to NO₂ and subsequent chemisorption as nitrites/nitrates on the perovskite surface.

In a previous study [23], the partial substitution of Ti by Cu in a BaTiO₃ perovskite allows obtaining a free-noble-metal catalyst (BaTi_{0.8}Cu_{0.2}O₃) with a NO_x Storage Capacity (NSC) at 420 °C similar to that shown by platinum-based catalysts (around 300 μmol/g.cat), which could be proposed as a potential component of high-temperature LNT systems for lean burn engines, such as Gasoline Direct Injection engines. The present paper aims to elucidate a mechanism for NO_x storage on this free-noble-metal catalyst (BaTi_{0.8}Cu_{0.2}O₃). Thus, the aim of this study is to determine the species formed under NO and NO/O₂ atmospheres (under temperature programmed and isothermal conditions) by in situ DRIFTS, as well as to correlate the results with the NO_x storage capacity of the catalyst. Finally, other ex situ characterization techniques have been used to try to identify the active phases for NO_x storage in the BaTi_{0.8}Cu_{0.2}O₃ catalyst.

2. Materials and Methods

2.1. Synthesis and Characterization of Catalysts

BaTi_{0.8}Cu_{0.2}O₃ catalyst was prepared using the Pechini sol-gel method [24] modified to be used in an aqueous media [24–26] as detailed elsewhere [23]. In brief, the titanium isopropoxide (Ti) was hydrolyzed and the resulting specie was solved in an aqueous solution of citric acid (CA) (Ti:CA = 1:2) and hydrogen peroxide (Ti:H₂O₂ = 2:1), forming a citrate-peroxo-titanate (IV) complex. Afterwards, the pH was dropwise adjusted to 8.5 with NH₃, and the barium (Ba:Ti = 1:1) and copper precursors, corresponding to the stoichiometry (BaTi_{0.8}Cu_{0.2}O₃), were added. The solution was kept at 65 °C for 5 h, until a gel was obtained. Then, the sample was dried at 90 °C for 24 h and, finally, calcined at 850 °C for 6 h.

The crystalline structure of the fresh and used catalyst was obtained by X-ray diffraction (XRD). X-ray diffractograms were recorded in a Bruker D8-Advance diffractometer (Berlin, Germany), using CuKα (0.15418 nm) radiation. Diffractograms were registered from 20 to 80° 2θ angles, with a step of 0.02° and a time per step of 3 s.

XPS were recorded using a K-Alpha Photoelectron Spectrometer from Thermo-Scientific with an AlKα (1486.6 eV) radiation source. The pressure of the analysis chamber was maintained at 5 × 10^{−10} mbar during XPS spectra recording. The binding energy (BE) and kinetic energy (KE) scales were adjusted setting the C1s transition at 284.6 eV, and the BE and KE values were then determined with the peak-fit software of the spectrometer.

Infrared spectroscopy analysis of the fresh and used samples was performed using a JASCO FT/IR 4700 spectrometer fitted with a DLATGS detector and an ATR Specac Golden Gate accessory. From these spectra, a semi-quantitative estimation of the percentage of barium carbonate in the fresh and used catalyst was carried out. For this analysis, $\text{BaTi}_{0.8}\text{Cu}_{0.2}\text{O}_3$ sample powder was mixed in an agate mortar with BaSO_4 using a 1:1 ratio. The spectra of the resulting powder mixture were recorded in the $4000\text{--}400\text{ cm}^{-1}$ range, with a 1 cm^{-1} resolution and as an average of 100 scans. From these spectra, the relationship between the intensities of the broad barium sulfate band, at $\sim 1060\text{ cm}^{-1}$, and the small peak due to BaCO_3 , at 860 cm^{-1} , ($I_{\text{BaSO}_4,1060\text{cm}^{-1}}/I_{\text{BaCO}_3,860\text{cm}^{-1}}$) was calculated. The percentage of BaCO_3 in the $\text{BaTi}_{0.8}\text{Cu}_{0.2}\text{O}_3$ catalyst was estimated, using a calibration curve drawn following identical procedure with $I_{\text{BaSO}_4,1060\text{cm}^{-1}}/I_{\text{BaCO}_3,860\text{cm}^{-1}}$ values measured from $\text{BaCO}_3:\text{BaSO}_4$ mixtures with different $\text{BaCO}_3:\text{BaSO}_4$ ratios.

The percentage of BaCO_3 present in fresh and used catalyst was also determined by thermogravimetric analysis using 30 mg of the fresh and used catalysts which was heated at $10\text{ }^\circ\text{C}/\text{min}$ from 25 to $900\text{ }^\circ\text{C}$ under a He flow ($100\text{ mL}/\text{min}$, $P_{\text{total}} = 1\text{ atm}$). These experiments were carried out in a TG-DTA device from Mettler-Toledo (model TGA/SDTA851e/LF/1600), fitted with a QMS (Quadrupole Mass Spectrometer, Pfeiffer Vacuum model Thermostar GSD301T).

2.2. NO_x Storage Tests

NO_x storage tests were performed in a fixed-bed reactor at atmospheric pressure under a gas flow of $500\text{ mL}/\text{min}$ ($\text{GSHV} = 30,000\text{ h}^{-1}$) containing either 500 ppm NO + 5% O₂ or 500 ppm NO in N₂. The catalytic bed was composed of 80 mg of catalyst and 320 mg of SiC. The gas composition was monitored by NDIR-UV gas analyzers for NO, NO₂, CO, CO₂ and O₂ (Rosemount Analytical Model BINOS 1001, 1004 and 1000). Temperature programmed reactions ($10\text{ }^\circ\text{C}/\text{min}$ from room temperature to $800\text{ }^\circ\text{C}$) were performed using the as-prepared catalyst. NO_x conversion profiles were determined as a function of temperature using the following Equation (2):

$$\text{NOx conversion (\%)} = \frac{\text{NOx}_{\text{in}} - \text{NOx}_{\text{out}}}{\text{NOx}_{\text{in}}} \times 100 \quad (2)$$

where “NO_{x,in}” is the concentration of NO_x (= NO + NO₂) fed to the reactor, while “NO_{x,out}” is the concentration of NO_x measured by the analyzers at the exit of the reactor.

The NSC was determined by carrying out ten consecutive storage–regeneration cycles at the selected temperatures by using the following procedure: (i) during the lean cycle (5 min) a gas flow ($500\text{ mL}/\text{min}$ ($\text{GSHV} = 30,000\text{ h}^{-1}$)) composed of 500 ppm NO and 5% O₂ balanced with N₂ was fed through the reactor while a rich gas flow (10% H₂ as model reductant in N₂ balance) was fed through a bypass path; (ii) at the required time, the gas paths were switched and during 3 min, the rich gas flow was fed into the reactor to regenerate the catalyst (rich cycle). This procedure was also carried out using a reactor without catalyst (400 mg of SiC), to determine the NO_{x,inlet} response of the gas analyzers. Please note that, although the time for rich and lean cycles is far from that of the real conditions, it allows determining the ability of the catalysts to store NO_x.

The NSC was calculated as the difference between the NO_x signal when the reactor is filled with SiC and the NO_x signal when the reactor is filled with the catalyst, by using Equation (3):

$$\text{NSC} = \int_{t_0}^{t_f} \text{NOx}_{\text{inlet}}(t) - \text{NOx}_{\text{exp}}(t) dt \quad (3)$$

where “NO_{x,inlet}” is the concentration of NO_x (= NO + NO₂) measured for the SiC filled reactor, and “NO_{x,exp}”, is the concentration of NO_x during the NO_x storage test.

2.3. In Situ Diffuse Reflectance Infrared Fourier Transform Spectroscopy (DRIFTS) Experiments

The analysis of species adsorbed on the catalyst surface during the NO_x storage experiments (both under temperature programmed reaction and isothermal conditions)

was carried out using a Shimadzu IRTracer-100 FTIR Spectrophotometer fitted with MCT detector. The instrumentation included Praying Mantis optics and a Harrick DRIFTS cell, which allowed heating of the samples to 550 °C. Spectra were recorded with a 4 cm⁻¹ resolution from 4000 to 400 cm⁻¹ and as an average of 16 scans. All catalysts were pretreated in the DRIFTS cell, at 450 °C for 30 min in a 500 ppm NO + 5% O₂ + N₂ atmosphere (100 mL/min), followed by 30 min in 10% H₂ + N₂ at the same temperature (regeneration step). Afterwards, the samples were cooled down to the desired temperature in N₂ atmosphere.

For temperature-programmed-reaction experiments, the preconditioned catalyst was heated at 10 °C/min from 50 to 500 °C and an IR spectrum was recorded every 50 °C. Five consecutive NO_x storage–regeneration cycles were carried out at 300, 350, 400 and 450 °C with the preconditioned catalyst and using lean (500 ppm NO + 5% O₂ balanced with N₂) and rich (10% H₂ balanced with N₂) 100 mL/min gas flows, respectively. As this paper is focused on the NO_x storage process, only the species formed during the lean cycle was followed by recording an IR spectrum every 30 s while the lean atmosphere was fed into the DRIFTS cell.

3. Results

3.1. Catalyst Characterization

A detailed discussion of the characterization results of the BaTi_{0.8}Cu_{0.2}O₃ has been presented elsewhere [23]. The more relevant characterization results are included in Figure S1a–d and Table S1 in the Supplementary Materials. Briefly, BaTi_{0.8}Cu_{0.2}O₃ catalyst synthesized by sol–gel method is a mixed oxide with perovskite structure (XRD) and negligible porosity. The XRD, XPS, and TPR-H₂ results revealed that copper has been incorporated into the BaTiO₃ perovskite structure with different electronic interaction with the lattice (and hence with different reducibility). The incorporation of copper into the structure generates oxygen vacancies, feasible active oxygen species for adsorption on the catalyst surface and, it induces both a pseudo distortion of the tetragonal structure (XRD and Raman Spectroscopy) and the segregation of some phases (mainly BaCO₃ and Ba₂TiO₄, but also a minor phase of CuO). As a consequence of all these modifications, active sites for the NO to NO₂ oxidation and for the NO_x storage are created on the copper-doped perovskites [23].

3.2. NO_x Storage under Temperature-Programmed Reaction Conditions

Figure 1a,b shows the NO_x conversion (calculated from Equation (2)) and the NO₂ generation profiles obtained for the BaTi_{0.8}Cu_{0.2}O₃ catalyst under both NO and NO/O₂ atmospheres. In these profiles, a positive value of NO_x conversion indicates that NO_x is stored on the catalyst as the NO_x concentration measured by the analyzers is lower than that fed into the reaction system, so, %NO_x conversion means %NO_x storage. On the contrary, a negative value of NO_x conversion reveals that NO_x has been desorbed, so in this case, %NO_x conversion represents %NO_x desorption [23]. A clear influence of the gas phase composition on the NO_x conversion profiles is observed. In a NO/O₂ atmosphere (red line), the NO_x conversion profile shows two adsorption maxima around 300–350 °C and 450 °C, and only one NO_x desorption peak at 550 °C. However, in NO/N₂ atmosphere (blue line), an almost flat NO_x conversion profile is found, suggesting that adsorption/desorption processes do not take place under these conditions.

To identify the species generated on the BaTi_{0.8}Cu_{0.2}O₃ catalyst as a function of temperature and atmosphere composition (NO/N₂ or NO/O₂), analogous temperature programmed reaction experiments were performed during in situ DRIFTS evaluation. The DRIFT spectra ranging from 1800 to 1000 cm⁻¹ are shown in Figure 2a,b, as it has been widely reported that this region corresponds with the wavenumber range where bands ascribed to nitrite/nitrate species can be identified [27], for instance, ionic (~1380 cm⁻¹), monodentate (1530–1480 cm⁻¹), bidentate (1565–1500 cm⁻¹) or bridged nitrates (1650–1600 cm⁻¹),

ionic ($\sim 1260\text{ cm}^{-1}$), monodentate ($1470\text{--}1450\text{ cm}^{-1}$) or bridged nitrites ($1220\text{--}1205\text{ cm}^{-1}$), and nitro compounds ($1470\text{--}1450\text{ cm}^{-1}$).

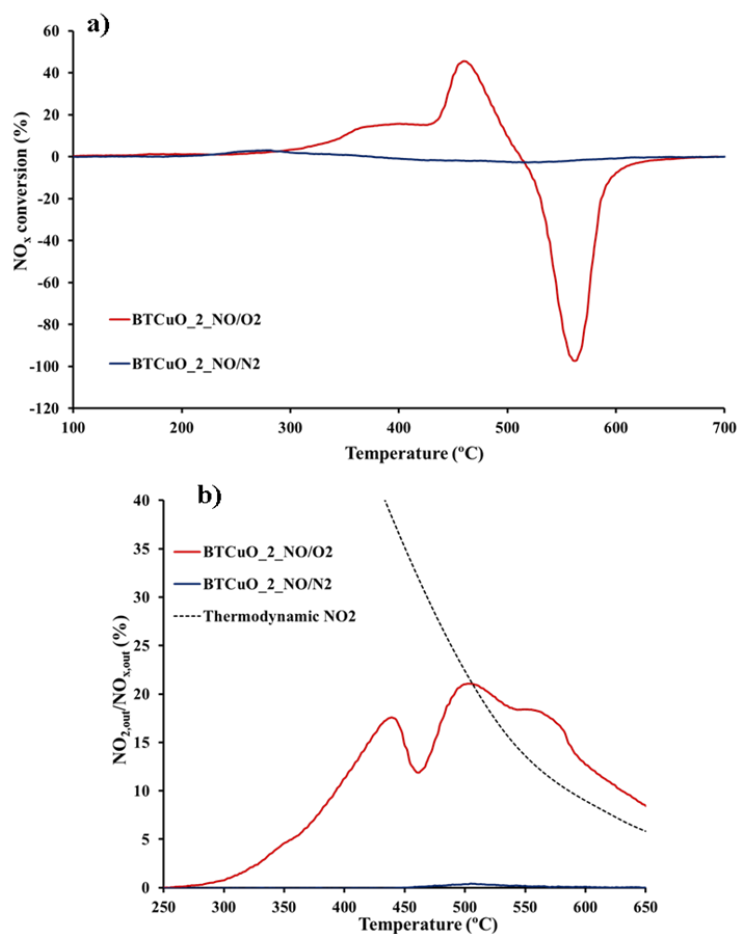


Figure 1. (a) NO_x conversion and (b) NO₂ generation profiles for BaTi_{0.8}Cu_{0.2}O₃ catalyst in 500 ppm NO + 5% O₂ and 500 ppm NO atmospheres under Temperature Programmed conditions.

All the DRIFT spectra show three main bands corresponding to carbonate groups present on the catalyst [28] (not labeled in Figure 2a,b) at 1055 , 1460 and 1760 cm^{-1} . The intensity of these bands was not affected by the pre-treatment of the catalyst, suggesting a high stability of these species. Considering that the broad band at 1460 cm^{-1} [29], overlaps with some of the bands corresponding to NO_x species and, also, the discrepancies published in literature related to the exact assignment of the different types of nitrate/nitrite species, in the subsequent discussion, the peaks detected in the DRIFT spectra will be assigned as barium nitrites or nitrates, thus, avoiding specific assignments among the different nitrogen species.

Under a NO/O₂ atmosphere (Figure 2a), a band at $1240\text{--}1220\text{ cm}^{-1}$ corresponding to barium nitrites [9,11,17] is identified at $100\text{ }^{\circ}\text{C}$. The intensity of this band increases with temperature up to $350\text{ }^{\circ}\text{C}$, when it achieves its maximum intensity. Beyond this temperature, the nitrites band starts to vanish, and new bands grow at 1040 , 1360 , 1540 and 1775 cm^{-1} ascribed to the formation of barium nitrates [15,30,31]. The latter bands become the only ones identified in the spectra recorded at 450 and $500\text{ }^{\circ}\text{C}$, confirming that barium nitrate is the final product in the NO_x storage process at high temperature. These results totally agree with previous studies concluding that, under a NO/O₂ atmosphere, the formation of nitrites on catalyst is the main route at low temperature, while at high temperature, these groups are oxidized to nitrates [5,11].

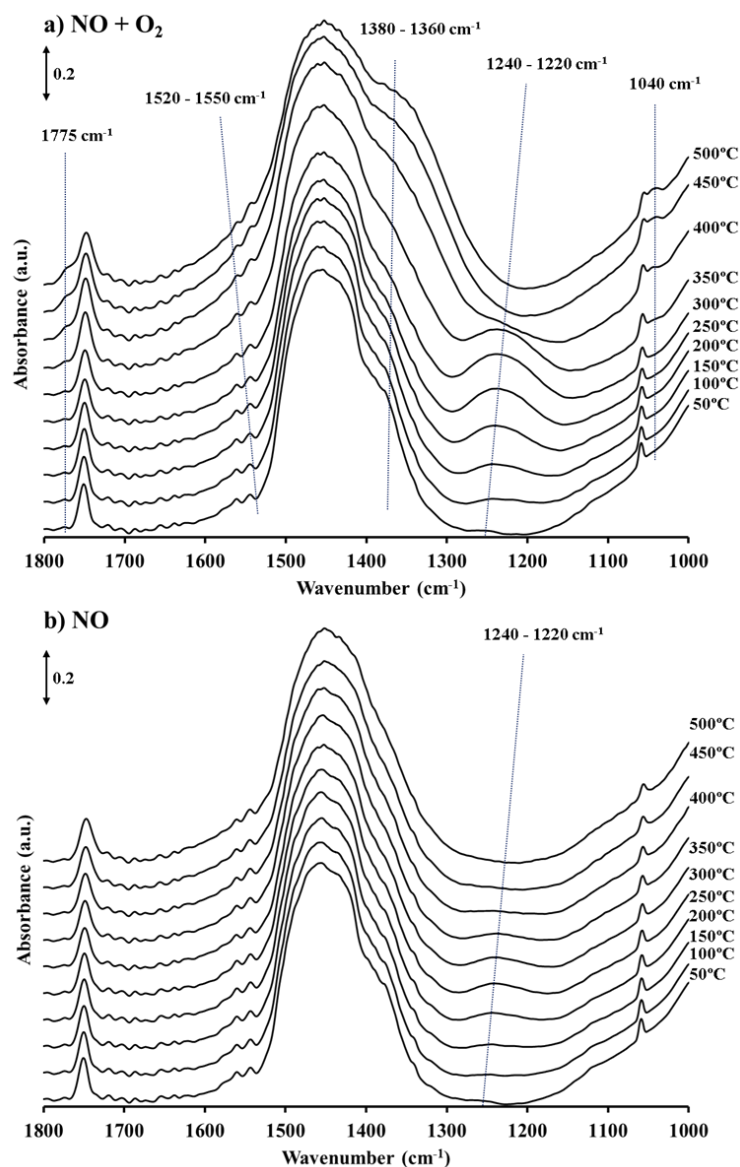


Figure 2. DRIFT spectra recorded under temperature programmed conditions in (a) 500 ppm NO + 5% O₂ and (b) 500 ppm NO atmosphere.

Two main differences are detected when compared the spectra recorded in a NO atmosphere (Figure 2b) with the former one. Firstly, bands ascribed to nitrites (1240–1220 cm⁻¹) are identified in spectra of the sample between 100 and 350 °C, but they show significantly lower intensity than under a NO/O₂ atmosphere (Figure 2a) indicating that in the absence of O₂, the NO_x storage capacity of the BaTi_{0.8}Cu_{0.2}O₃ perovskite is much lower or almost negligible, which agrees with NO_x conversion profiles (Figure 1b). Secondly, in the DRIFT spectra recorded above 350 °C, nitrite bands disappear (as observed in the presence of O₂) but peaks corresponding to barium nitrates are not clearly detected. The decrease in the intensity of the nitrite band suggests that these groups are unstable above 350 °C in absence of O₂ in the atmosphere; however, partial oxidation of nitrites to nitrates may not be ruled out although the nitrate bands could not clearly be detected [29].

3.3. NO_x Storage under Isothermal Reaction Conditions

Cyclic NO_x storage–regeneration experiments were carried out under NO/O₂ between 300 and 450 °C (temperature range at which the BaTi_{0.8}Cu_{0.2}O₃ catalyst shows NO_x storage capacity according to Figure 1a).

Table 1 shows the amount of NO_x stored (as NSC, NO_x Storage Capacity, in μmol/g. catalyst) on the catalyst at different temperatures, calculated as the difference between the NO_x signals when the reactor is filled with SiC (inert material) and filled with catalyst.

Table 1. NO_x storage capacity (NSC) of the BaTi_{0.8}Cu_{0.2}O₃ catalyst at different temperatures in 500 ppm NO + 5% O₂ balanced with N₂.

Temperature (°C)	NSC (μmol/g.cat.)	NO ₂ /NO _x (%)
300	211	5
350	231	11
400	262	16
450	340	15

Please note that, as expected [23], NSC increases with temperature. It is widely accepted that NO₂ is the main species adsorbed on an NSR catalyst, so, direct correlation exists between NO₂ generation activity and NSC. In agreement with this, in the BaTi_{0.8}Cu_{0.2}O₃ catalyst, the highest NSC is achieved at the temperature range in which this catalyst shows its highest NO to NO₂ oxidation activity (Figure 1b). It is remarkable that the NSC featured by the BaTi_{0.8}Cu_{0.2}O₃ catalyst is within the range of values expected for NSR application, even though the temperature is higher than those reported for model NSR catalysts, for this reason, it has been suggested that this new material might be of interest for high-temperature applications, as in GDI engines [23].

Analogous cyclic NO_x storage–regeneration experiments were carried out with the BaTi_{0.8}Cu_{0.2}O₃ catalyst in a DRIFTS cell to determine the species formed during NO_x storage. The DRIFT spectra were registered at 30 s time intervals, once the lean atmosphere (composed of 500 ppm of NO, 5% of O₂ in N₂) was fed. To ensure catalyst regeneration, a 10% H₂ in N₂ (rich conditions) was used during the regeneration cycle.

Figure S2a–d (Supplementary Materials) shows the DRIFT spectra obtained during the NO_x storage cycles. These spectra show that, at any temperature, the amount of NO_x species on the catalyst surface increases with time on NO/O₂ stream. However, due to the short time of the storage-cycle and likely overlapping with the carbonate bands, some of the signals ascribed to nitrates and nitrites might be hard to identify. Thus, in order to clarify the analysis, only the evolution in the intensity of two selected bands was followed during NO_x exposure: (i) 1240–1220 cm^{−1} for nitrites, and (ii) 1380–1360 cm^{−1} for nitrates. In Figure 3a,b, the difference between the absorbance values (after baseline correction) recorded every 30 s and the absorbance value registered once the switch from rich to lean conditions is carried out (i.e., at t = 0 s) is shown as a function of time and for each reaction temperature (300, 350, 400 and 450 °C). As observed under temperature-programmed reaction conditions, at low temperature (300 °C) the NO_x storage takes place forming nitrites and nitrates. Thus, at 300 °C, the intensity of the nitrites band (Figure 3a) increases during the early stages of exposure to NO/O₂ (~90 s), but longer time on stream involves a depletion of nitrites followed by an increase of the nitrate bands (Figure 3b). As the storage temperature increases, two clear effects can be noticed:

1. At 350 and 400 °C, the lifetime of the nitrite species, formed at the beginning of the NO_x storage cycle, becomes shorter. Thus, the intensity of the nitrite band increases until 30 s of NO/O₂ exposition and, afterwards, the nitrite band intensity drastically drops. This trend suggests that the oxidation of nitrites to nitrates becomes faster at these temperatures than at 300 °C. In fact, at 450 °C, nitrites are not detected even at the very beginning of the NO_x storage step.
2. A significant increase in the intensity of the nitrates band (Figure 3b) is detected as the storage temperature rises, which can be directly related to the increase of the NSC (Table 1).

Thus, in situ DRIFTS results obtained under isothermal conditions confirms that, between 300 and 400 °C, nitrites and nitrates coexist on the catalyst but, as the temperature

increases, nitrite oxidation to nitrates become faster and consequently, only nitrates are detected at higher temperature (450 °C).

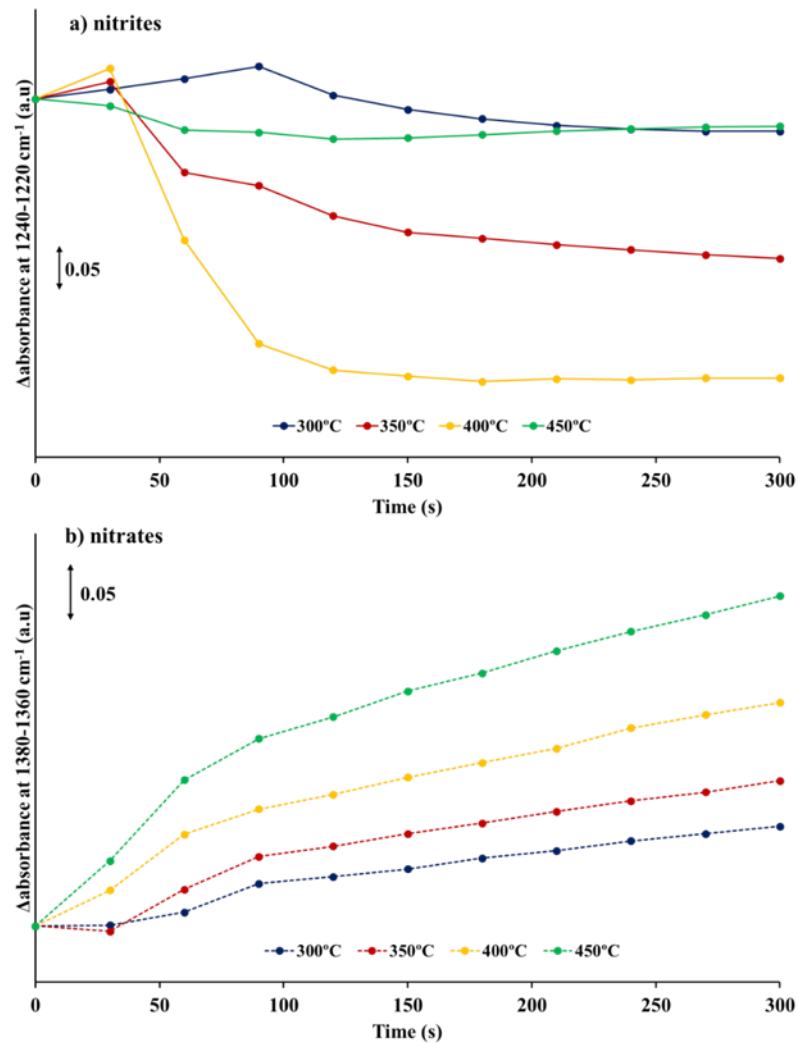


Figure 3. Evolution of intensity of absorbance bands ascribed to (a) nitrites (1240–1220 cm⁻¹) and (b) nitrates (1380–1360 cm⁻¹) obtained from the DRIFT spectra shown in Figure S2a–d.

3.4. Identification of Active Phase for NO_x Storage

XRD was used to determine any effect of NO_x storage on the perovskite structure of the BaTi_{0.8}Cu_{0.2}O₃ catalyst. Additionally, this technique may help to identify the role of the BaCO₃ or Ba₂TiO₄ segregated phases (identified in the XRD patterns of the fresh catalyst) in the NO_x storage process. Figure 4 compares the XRD pattern of the fresh BaTi_{0.8}Cu_{0.2}O₃ catalyst with the diffractograms recorded after two different ex-situ pretreatments: (i) 1 h exposure to NO_x at 400 °C using an atmosphere composed of 500 ppm NO + 5% O₂ balanced with N₂, to simulate catalyst saturation (called BTCuO_2_sat), and (ii) 1 h under an NO/O₂ atmosphere at 400 °C followed by 1 h under rich conditions (10% H₂/N₂), for reproducing the regenerated catalyst, called BTCuO_2_red. It is worth mentioning that, for this analysis, longer time pretreatments have been used since XRD characterization does not allow the detection of surface phases, therefore, under these new conditions, the generation of bulk and crystalline phases was guaranteed.

The XRD pattern of the fresh BaTi_{0.8}Cu_{0.2}O₃ catalyst shows that tetragonal BaTiO₃ perovskite is the main phase in this catalyst, while the incorporation of copper induces the segregation of mainly BaCO₃ and Ba₂TiO₄, but also CuO phases [23] (denoted as BTCuO_2 in Figure S1a in Supplementary Materials). After the first 1 h NO_x storage pretreatment

(BTCuO_2_sat), the perovskite structure remains as the main phase; however, the peaks corresponding to the Ba_2TiO_4 phase disappear and new diffraction signals ascribed to $\text{Ba}(\text{NO}_3)_2$ [32] and BaCO_3 are identified. These changes in the diffraction pattern suggest that the segregated Ba_2TiO_4 phase is acting as an NO_x storage phase in NO/O_2 atmosphere, forming barium nitrates. It is worth mentioning that, although BaCO_3 is observed in the XRD pattern of the as prepared catalyst, the higher intensity of the carbonate reflection for BTCuO_2_sat may be attributed to further carbonation of barium nitrates during the exposure of the catalyst to atmospheric CO_2 before recording the XRD pattern.

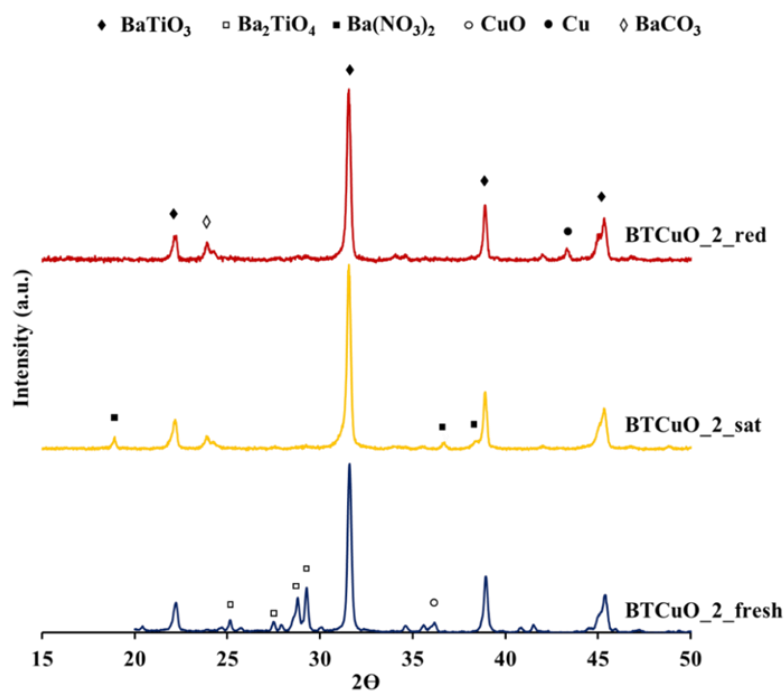


Figure 4. XRD patterns recorded for the as-prepared $\text{BaTi}_{0.8}\text{Cu}_{0.2}\text{O}_3$ catalyst (BTCuO_2_fresh), after 1 h of NO_x exposure in 500 ppm $\text{NO} + 5\% \text{O}_2$ in N_2 atmosphere (BTCuO_2_sat) and finally after regeneration in 10% H_2/N_2 atmosphere (BTCuO_2_red).

In the XRD pattern registered after catalyst regeneration (BTCuO_2_red), the perovskite structure is still the main phase, so, even after a regeneration cycle, the structure does not collapse. In this pattern, peaks ascribed to barium nitrate are not identified, confirming that nitrates are removed during the regeneration cycle. However, as peaks corresponding to the Ba_2TiO_4 phase are neither detected, it seems that the regeneration of the Ba_2TiO_4 phase does not occur after barium nitrate removal. Additionally, the increase in the intensity of the BaCO_3 peaks with respect to the BTCuO_2_sat suggests that barium nitrate decomposition leads to the formation of BaO phase, which is identified as barium carbonate by XRD due to the carbonation after exposure to the atmospheric CO_2 . Please note that a new diffraction peak assigned to metallic copper is also observed in the BTCuO_2_red pattern. Considering the rich cycle conditions of this pretreatment (10% H_2/N_2 at 400 °C), this peak is consistent with catalyst reducibility [23] (Figure S1d in Supplementary Information).

The percentage of barium carbonate for the $\text{BaTi}_{0.8}\text{Cu}_{0.2}\text{O}_3$ catalyst at the different stages of the NO_x storage–regeneration process was assessed using Attenuated Total Reflectance spectroscopy (ATR), thermogravimetric analysis (TGA) and XPS techniques. For this evaluation, in order to conditioning the catalyst, three different pretreatments were performed: (i) five NO_x storage–regeneration cycles at 400 °C called BTCuO_2_NSR, (ii) five NO_x storage–regeneration cycles at 400 °C followed by 1 h in NO/O_2 atmosphere at the same temperature for simulating catalyst saturation, called BTCuO_2_sat, and (iii) five NO_x storage–regeneration cycles at 400 °C followed by 1 h in NO/O_2 atmosphere and,

subsequently, 1 h regeneration under rich conditions (to reproducing a regenerated catalyst surface situation), called BTCuO_2_red. The results of this estimation of barium carbonate by these three techniques are listed in Table 2.

Table 2. Estimation of the BaCO₃ percentage by ATR, TGA, and XPS (atomic C percentage).

Catalyst	ATR (w/w %)	TGA (w/w %)	XPS (w/w % of C)
BTCuO_2_NSR	7.7	5.6	3.5
BTCuO_2_sat	4.9	4.9	1.9
BTCuO_2_red	6.5	5.8	2.7

In the DRIFT spectra of the fresh BaTi_{0.8}Cu_{0.2}O₃ catalyst, three bands at 1055, 1460 and 1760 cm⁻¹, assigned to barium carbonate, are identified. Figure 5 shows the DRIFT spectra recorded after the three described pretreatments. In agreement with XRD, carbonates are still detected for BTCuO_2_sat and for BTCuO_2_red proving the high stability of these species under experimental conditions. However, bands corresponding to nitrates (blue dotted lines) are only detected for BTCuO_2_sat, confirming that NO_x stored on the catalyst is taking place by forming nitrates as final product. As these nitrate bands are not identified after the NO_x storage–regeneration cycles (i.e., reduction pretreatments), the total regeneration of the catalyst is confirmed.

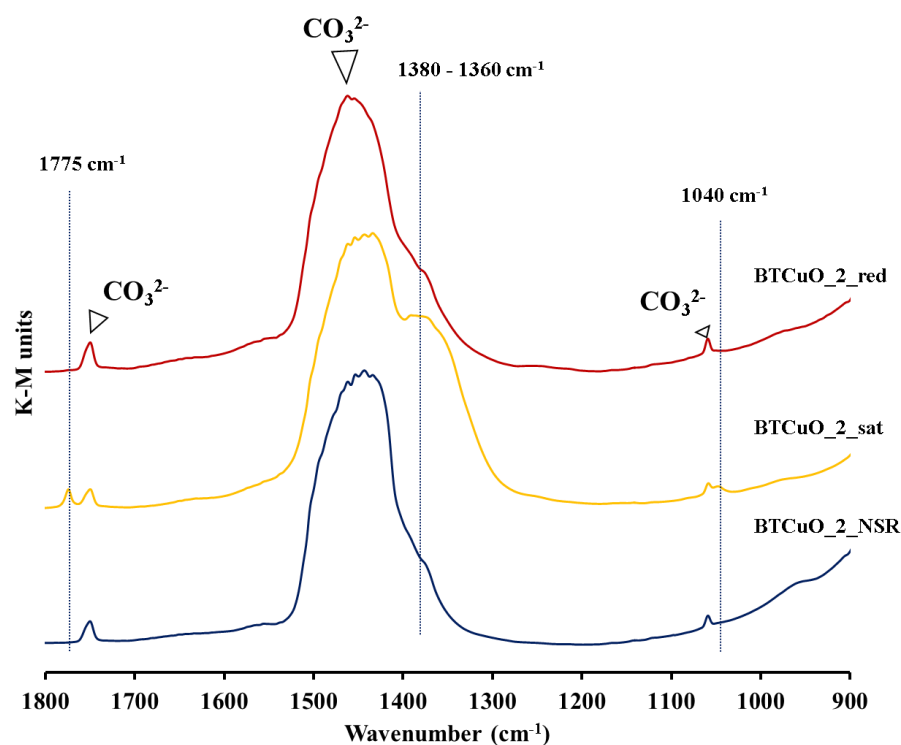


Figure 5. DRIFT spectra for the BaTi_{0.8}Cu_{0.2}O₃ catalyst after 5 NO_x storage–reduction cycles (BTCuO_2_NSR), followed by 1 h NO_x exposure experiment in 500 ppm NO + 5% O₂ in N₂ (BTCuO_2_sat) and finally regeneration in 10% H₂/N₂ (BTCuO_2_red).

Despite significant visual changes in the intensity of the carbonates band at ~1460 cm⁻¹ are not observed in the spectra (Figure 5), ATR spectroscopy has been used for estimating the percentage of carbonate remaining after every pretreatment (see Experimental Section for details). Data in Table 2 show that the percentage of barium carbonate decreases after NO_x uptake experiments, confirming that carbonates are removed from the catalyst during No_x exposure because they are displaced by NO_x, leading to nitrates as a final product (Figure 5). After catalyst regeneration (BTCuO_2_red), a recovery of the carbonate

percentage due to the adsorption of atmospheric CO₂ on the BaO phase, formed from barium nitrate decomposition, is found.

The weight loss profiles, obtained in a TG experiment carried out up to 900 °C and using 100 mL/min He gas flow, are shown in Figure 6. The weight losses at high temperature (maximum slope at approximately 815 °C) are listed in Table 2. This weight loss is due to the BaCO₃ decomposition to BaO and CO₂, since an intense signal corresponding to CO₂ release ($m/z = 44$ and 28) was detected by a QMS at this temperature (not shown). Please note that in the TGA profile of the BTCuO_2_sat catalyst, a weight loss is observed between 450 and 550 °C, which corresponds to desorption of the previously adsorbed NO_x (Figure 1) during the NO_x storage pretreatment (a release of NO ($m/z = 30$) and O₂ ($m/z = 32$), (not shown), was detected by QMS at that temperature). In Table 2, the trend in the BaCO₃ percentage determined by TGA after the different pretreatments is similar to that shown by ATR spectroscopy, i.e., a decrease in barium carbonate percentage after exposure to NO_x, and an increase in this value after the regeneration pretreatment. This fact supports carbonates being released from the BaTi_{0.8}Cu_{0.2}O₃ catalyst during NO_x storage and regenerated after CO₂ atmospheric exposure, once NO_x is removed from the catalyst after the regeneration pretreatment.

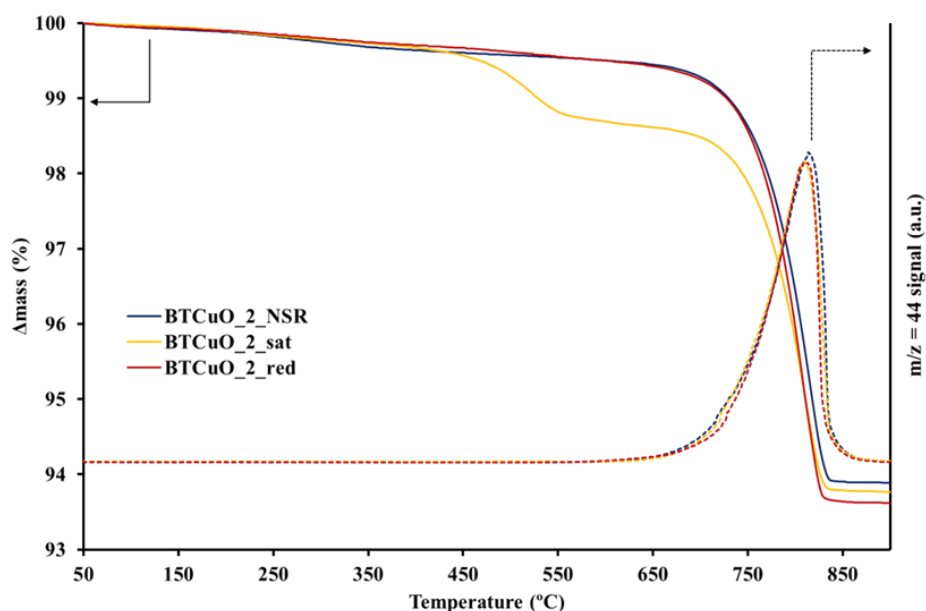


Figure 6. TGA and $m/z = 44$ profiles in He of the BaTi_{0.8}Cu_{0.2}O₃ catalyst after 5 NO_x storage-reduction cycles (BTCuO_2_NSR), followed by 1 h NO_x exposure to 500 ppm NO + 5% O₂ in N₂ (BTCuO_2_sat) and finally reduced in 10% H₂/N₂ (BTCuO_2_red).

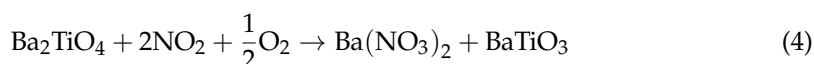
The atomic percentage of Ba, Ti, O, Cu and C on the surface of the BaTi_{0.8}Cu_{0.2}O₃ catalyst after the three pretreatments was determined by XPS from the signals corresponding to the Ba3d_{3/2}, Ti2p_{3/2}, O1s, and Cu2p_{3/2}, and C1s transitions, respectively. From the Ba and O profiles, the presence of carbonates on the catalyst surface is proven. In general, the C1s transition is used in XPS analysis as a standard reference for setting the XPS transitions of the other elements, since carbon (hydrocarbon) is a common impurity in most of the materials under ultra-high-vacuum conditions (284.6 eV) [33]. For the BaTi_{0.8}Cu_{0.2}O₃ catalyst, the C1s transition showed a shoulder at ~289–290 eV (Figure S3 in Supplementary Information) which is associated with the presence of carbonate groups [34]. Thus, the percentage of C due to carbonates was calculated from the area of this peak, after recalculating the quantities of all the elements present in the sample by correcting the contribution of carbon impurities (Table 2). As observed by ATR and TGA (which determines bulk carbonates), the percentage of C ascribed to the presence of surface is lower for BTCuO_2_sat than for BTCuO_2_NSR and grows during regeneration (BTCuO_2_red).

4. Discussion

The aim of this study is to analyze the NO_x storage process on a BaTi_{0.8}Cu_{0.2}O₃ catalyst from a mechanistic point of view. The results show that, as a model NSR catalyst [7], nitrites and nitrates are formed in the BaTi_{0.8}Cu_{0.2}O₃ catalyst when exposed to a NO/O₂ atmosphere.

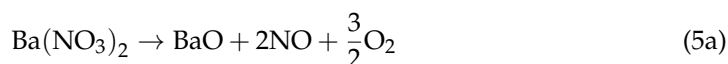
The characterization results revealed that the introduction of copper into the perovskite lattice originates a pseudo distortion of the structure, but also the segregation of phases such as Ba₂TiO₄ and BaCO₃. The formation of Ba₂TiO₄ is identified as an intermediate in the synthesis of BaTiO₃ from BaCO₃ and TiO₂ reaction by ceramic method [35–39]. Some of these studies conclude that Ba₂TiO₄ is formed in the reaction zone between TiO₂ and BaCO₃ such that at the end of the process a thin layer on the BaTiO₃ surface may remain. In agreement with this conclusion, the XPS (Cu + Ti)/Ba ratio in Table S1 (calculated from the atomic percentage of Cu, Ti and Ba) shows the surface barium enrichment due to the presence of Ba₂TiO₄ as a segregated phase [23].

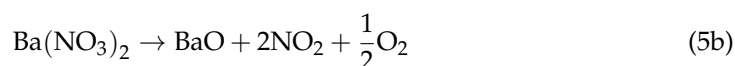
XRD patterns (Figure 4) of sample after exposure to a NO/O₂ atmosphere at 400 °C, reveal that Ba₂TiO₄ mixed oxide acts as an active phase for NO_x storage because, at this temperature and after 1 h exposure, peaks corresponding to this phase totally disappear and new peaks assigned to Ba(NO₃)₂ are detected [32]. Szanyi et al. [40] analyzed by TR-XRD the NO₂ uptake process on a BaO/Al₂O₃ catalyst after 5 min of exposure to NO₂ at different temperatures. In this analysis, they detected peaks corresponding to barium nitrates and the decrease in the intensity of BaO diffraction peaks during the experiment. On the basis of this result, the authors concluded that NO₂ storage leads to the formation of bulk barium nitrates that transforms the BaO phase. Please note that, at 400 °C, the BaTi_{0.8}Cu_{0.2}O₃ catalyst shows a high NO to NO₂ oxidation activity (Figure 1b); therefore, the transformation of Ba₂TiO₄ into barium nitrates seems to take place when high NO₂ concentrations are present in the gas phase. This suggests that NO₂ is being consumed by following Reaction (4):



Templeton and Pask [37] and Beauger et al. [41] demonstrated that the CO₂ partial pressure has a key role on the presence of the intermediate Ba₂TiO₄ phase during BaTiO₃ synthesis by the ceramic method. Both studies concluded that CO₂ reacts with the intermediate Ba₂TiO₄ at high temperatures leading to the formation of barium carbonate and barium titanate as final products. Considering the competition between CO₂ and NO₂ for the basic oxide sites of a NSR model catalyst [42,43], despite different acidities of CO₂ and NO₂, it may be assumed that the NO_x storage follows the previously proposed Reaction (4).

After the regeneration pretreatment, XRD peaks of the barium nitrate disappears due to desorption of the previously stored NO_x species, thus, indicating that the removal of them from the catalyst is achieved during the rich cycle. However, as the diffraction peaks corresponding to the Ba₂TiO₄ phase are not detected after nitrate decomposition, it seems that Ba₂TiO₄ is not formed again. Accordingly, peaks ascribed to the presence of BaCO₃ phase are clearly identified with a higher intensity than that observed after the NO_x adsorption process. By TR-XRD [40], it has been demonstrated that barium nitrate decomposition in an inert atmosphere leads to the formation of barium oxide. As BaO is readily carbonated due to the exposure to air, it can be concluded that, after the regeneration cycle, barium oxide is formed as a primary product of barium nitrate decomposition. During the NO_x storage experiment under temperature programmed conditions, NO and NO₂ are detected at NO_x desorption temperatures (Figure S4 in Supplementary Information). Thus, the following two reactions account for nitrate decomposition pathways (5a,b)





Reactions (5a,b) show the barium nitrate decomposition process and, consequently, the barium oxide formation, which is indirectly identified by XRD as barium carbonate. However, it cannot be ruled out that, due to the presence of H_2 during the reduction pretreatment, NO and NO_2 can be also partially reduced to nitrogen instead of being only desorbed in the form of nitrogen oxides.

In summary, it can be concluded that Ba_2TiO_4 is an active phase for NO_x storage from a NO/O_2 atmosphere, forming barium nitrate and barium titanate. However, this is an irreversible process that leads to BaO formation after nitrate decomposition, instead of Ba_2TiO_4 regeneration. Thus, BaO, which is originated from Ba_2TiO_4 , seems to be the active phase for NO_x storage in this catalyst when performing in cycling conditions after first NO_x adsorption step. Therefore, during the first NO_x storage cycle using the as-prepared $\text{BaTi}_{0.8}\text{Cu}_{0.2}\text{O}_3$ catalyst, Ba_2TiO_4 would act as a NO_x storage site during the rich stage and, during regeneration, BaO would be formed by barium nitrate decomposition which becomes the active site for NO_x storage in subsequent NO_x storage–regeneration cycles.

Based on these conclusions, the relevance of the BaO phase generated after the removal of NO_x from the catalyst surface as a NO_x storage site was analyzed in detail. For this purpose, the changes in the percentage of barium carbonate present in the catalyst after the different pretreatments (after five NO_x storage–reduction cycles at 400 °C, after 1 h NO_x exposure in NO/O_2 , and also after the reduction of the saturated catalyst under rich conditions for 1 h) was determined by ATR, TGA and XPS. BaCO_3 was selected from these analyses as it is formed during exposure of pretreated catalyst to atmospheric air [44]. Even though these techniques can be considered as reliable for carbonate identification purposes, Blanco-López et al. [45] demonstrated that it is difficult to assess quantitatively the amount of BaCO_3 in BaTiO_3 at low carbonate levels. Accordingly, only the changes in the percentage of carbonate from a semi-quantitative point of view have been discussed. The percentage of barium carbonate measured by ATR, TGA and XPS, and it is worth indicating that these three values are different for the following reasons: (i) only surface carbonate is determined by XPS, (ii) bulk carbonate is measured by TGA, and (iii) the amount of carbonate estimated by ATR could be surface or bulk depending on the experimental conditions (light-beam penetration). Despite of the differences between these three techniques, all data obtained from them (included Table 2) reveal that the percentage of barium carbonate in the $\text{BaTi}_{0.8}\text{Cu}_{0.2}\text{O}_3$ catalyst is lower after NO_x saturation (long NO_x adsorption cycle) than after NO_x storage (short NO_x adsorption cycle), which indicates that during adsorption process, NO_x displace carbonates generating nitrates that, at the end, are detected by DRIFTS (Figure 5). Please note that these nitrates are not completely removed from the catalyst due to exposure to atmospheric CO_2 , indicating their high stability. After catalyst reduction, in 10% H_2/N_2 , nitrates are removed, and the catalyst is regenerated. As a consequence, barium oxide is formed which is subsequently carbonated due to the adsorption of CO_2 from the exposition to atmospheric air [44]. In ATR, TGA and XPS data this fact is translated in an increase in the barium carbonate content after the 10% H_2/N_2 regeneration step.

In brief, as a result of the incorporation of copper into the perovskite structure, Ba_2TiO_4 is generated which, after NO_x storage–regeneration cycles, is converted to BaO that becomes relevant for NO_x storage in the $\text{BaTi}_{0.8}\text{Cu}_{0.2}\text{O}_3$ catalyst. Obviously, NO_x storage on the perovskite cannot be ruled out (considering that NO_2 storage on barium perovskites has been reported [20,21,46]), but the low specific surface area of the catalyst under study and also the reported negative effect that the formation of $\text{Ba}_x\text{Ti}_y\text{O}_z$ perovskite has on the NSC of a model $\text{BaO}/\text{TiO}_2/\text{Al}_2\text{O}_3$ [47] support that the role of the perovskite on NO_x storage is not significant.

According to the literature, a large controversy exists related to the formation of $\text{Ba}_2\text{TiO}_4/\text{BaCO}_3/\text{BaO}$ as a thin layer on the surface or as discrete particles during BaTiO_3 synthesis. In analogous TG experiments, Blanco-López et al. [45] did not identify any

weight loss associated with the decomposition of surface BaCO_3 in BaTiO_3 mixed oxides at the relatively low temperatures observed in this study. They concluded that barium carbonate decomposition is controlled by the partial pressure of CO_2 at those temperatures [37] and it may be assumed to be a very slow process that could not be properly identified by TGA. Piacentini and co-workers [48] demonstrated that the high amounts of barium oxide lead to the formation of bulk-like barium carbonate, with high thermal stability and low activity for NO_x storage. In $\text{BaTi}_{0.8}\text{Cu}_{0.2}\text{O}_3$ catalyst, the low temperature for barium carbonate decomposition and the high NO_x storage capacity indicate that this barium carbonate is very reactive, so it should be located at the catalyst surface. On the basis of the above results, a representation of the phases present in the $\text{BaTi}_{0.8}\text{Cu}_{0.2}\text{O}_3$ catalyst is shown in Figure 7.

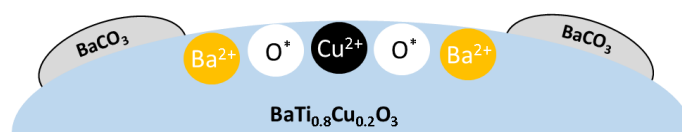
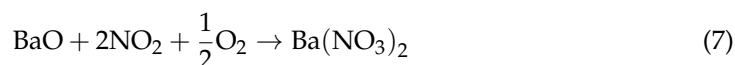


Figure 7. Composition of the $\text{BaTi}_{0.8}\text{Cu}_{0.2}\text{O}_3$ perovskite-type catalyst under reaction conditions.

Once the active phases have been identified, the NO_x storage mechanism can be carefully addressed. Two different temperature regions can be distinguished in the in situ DRIFTS experiments carried out under temperature-programmed conditions (Figure 2). Below 350°C , NO_x is stored on the catalyst as nitrites, while above this temperature, nitrites disappear and bands corresponding to nitrates are detected. This trend is in agreement with the two proposed routes for the NO_x storage on alkaline oxides [5,10,11]: (i) adsorption of NO and fast oxidation by O_2 forming nitrites that are subsequently oxidized to nitrates, called the “nitrite route”, and (ii) the formation of nitrates through the adsorption of NO_2 (obtained from NO oxidation to NO_2), called the “nitrate route”.

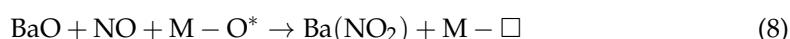
As above 350°C , $\text{BaTi}_{0.8}\text{Cu}_{0.2}\text{O}_3$ shows its highest NO to NO_2 oxidation activity (Figure 1b), it can be assumed that the NO_x storage mechanism proceeds as follows: (i) oxidation of NO to NO_2 on the perovskite surface (6), since the copper present in the catalyst is active for NO to NO_2 oxidation under an NO/O_2 atmosphere, followed by (ii) NO_2 adsorption as nitrates on the barium oxide located at the $\text{BaTi}_{0.8}\text{Cu}_{0.2}\text{O}_3$ catalyst surface (7):



It is generally accepted that NO_2 is the main species stored on a model NSR catalyst [1]. Fridell et al. [5] proposed that the adsorption of NO_2 involves a pathway in which the adsorption of three molecules of NO_2 implies the desorption of one molecule of NO , by following the general Equation (1). The NO_2/O_2 adsorption–desorption experiments under temperature programmed conditions (Figure S4 in Supplementary Information) revealed that NO is released at the NO_2 adsorption temperatures. Thus, it seems that the disproportionation mechanism (Equation (1)) takes place for NO_2 storage on the $\text{BaTi}_{0.8}\text{Cu}_{0.2}\text{O}_3$ catalyst.

Below 350°C , nitrites are the main NO_x species identified by DRIFTS for the $\text{BaTi}_{0.8}\text{Cu}_{0.2}\text{O}_3$. Similar results were obtained by Lietti et al. [11], who considered nitrite formation to be a dominant pathway in the NO_x storage process at low temperature for model NSR catalysts under NO/O_2 . These authors concluded that, at low temperature, NO is partially oxidized by O_2 in the noble metal–alkaline oxide border and, subsequently, stored forming nitrite and avoided overoxidation of NO to NO_2 . Hence, the so-called “nitrite route” implies good contact between oxidation and storage sites but also requires that oxidation sites acts as a supplier of oxygen to BaO , which promotes the NO to nitrites oxidation.

To determine the activity of the catalyst for NO storage, NO adsorption experiments without O₂ in the reaction gas composition were also carried out. In Figure 1b, NO₂ is not detected at any temperature under NO/N₂. Under this condition, the detection of nitrites (Figure 2b) by DRIFTS reveals that NO must be adsorbed on BaTi_{0.8}Cu_{0.2}O₃, predominantly on BaO sites of the catalyst. As O₂ is absent in this experiment, the perovskite must supply the oxygen needed for the NO to nitrite oxidation step. The characterization results previously discussed, allow concluding that the introduction of copper into the perovskite structure leads to an increase in oxygen vacancies and oxygen surface groups in the catalyst structure. Thus, this surface-active oxygen, and also the presence of a reducible cation (copper), facilitate oxidation of NO to nitrite. This assumption requires a good contact between the adsorption sites and the oxidation sites, suggesting that BaO has to be located on the surface of the BaTi_{0.8}Cu_{0.2}O₃ catalyst. These results allow concluding that NO is also adsorbed by forming nitrites according to Equation (8):



where M–O* is an oxidation active site, which could be either an activated oxygen site on the perovskite surface formed by the adsorption of O₂ at an oxygen vacancy or a copper active site (M=Cu) and, M–□ is an oxygen vacancy generated due to oxygen consumption.

Evidence for both “nitrite” and “nitrate” routes has been observed in cyclic NO_x storage-regeneration experiments carried out by DRIFTS at 300, 350, 400 and 450 °C with the BaTi_{0.8}Cu_{0.2}O₃ catalyst (Figure S2a–d in Supplementary Information). Under isothermal conditions, the dominant NO_x storage route is also highly dependent on the temperature. At low temperature (300 °C), NO_x is adsorbed as nitrite on the perovskite catalyst during the initial stages of the NO_x storage cycle; however, these nitrites show a short lifetime, and after ~90 s, the bands corresponding to nitrites start to disappear, as these species are oxidized to nitrates by O₂. Afterwards, only nitrates are detected as NO_x stored species. By increasing the temperature, the lifetime of the nitrite species decreases and, at 450 °C, these species are no longer identified at the initial stages of the NO_x storage indicating that the nitrite to nitrate oxidation step is promoted by increasing the temperature. As previously shown, the activity of catalyst for oxidation increases with temperature, thus favoring the fast oxidation of nitrites to nitrates, so, nitrites are not identified even at the beginning of the NO_x storage cycle. Additionally, at high temperatures, NO₂ generation is also improved, promoting the direct NO₂ adsorption to form nitrates (nitrates route).

In summary, in situ DRIFTS experiments revealed that, for model NSR catalysts, NO_x storage on BaTi_{0.8}Cu_{0.2}O₃ catalyst takes place by both “nitrite” and “nitrate” routes, with the dominant pathway being highly dependent on the catalyst temperature and time on stream. At low temperatures (T < 350 °C), nitrites are formed on the catalyst, and are subsequently oxidized to nitrates. Above 350 °C, the high oxidation activity of the perovskite promotes the nitrite to nitrate oxidation and the NO₂ generation and, consequently, the nitrate route prevails.

5. Conclusions

The incorporation of copper into the BaTi_{0.8}Cu_{0.2}O₃ perovskite structure induces a segregation of predominantly BaCO₃ and Ba₂TiO₄, but also CuO. XRD shows that Ba₂TiO₄ is an active phase for NO_x storage, forming barium titanate and barium nitrate as final products. However, after nitrate decomposition, BaO is generated on the catalyst surface instead of Ba₂TiO₄. The estimation of the amounts of BaCO₃ by ATR, TGA and XPS reveals that this BaO plays a key role during the NO_x storage process on the BaTi_{0.8}Cu_{0.2}O₃ catalyst.

Nitrites and nitrates are detected for the BaTi_{0.8}Cu_{0.2}O₃ catalyst by in situ DRIFTS experiments under temperature programmed conditions and NO_x storage–regeneration cycles at different temperatures. This fact indicates that, as for model NSR catalysts, both “nitrite” and “nitrate” routes take place during the NO_x storage process.

A strong correlation between the oxidation activity of the perovskite and the NO_x storage were observed. At low temperature ($T < 350$ °C) nitrites are formed on the catalyst by NO adsorption which are subsequently oxidized to nitrates, due to the participation of activated oxygen and copper (as redox active metal) on the perovskite surface. Above this temperature, the high oxidation activity shown by the catalyst enhances NO₂ generation and the role of the nitrate route in the NO_x storage mechanism. Additionally, this high oxidation activity promotes the nitrites to nitrates oxidation. Thus, as for model NSR catalysts, it can be concluded that the dominant pathway for NO_x storage on BaTi_{0.8}Cu_{0.2}O₃ catalyst is highly dependent on the catalyst temperature and on the time on stream.

Supplementary Materials: The following are available online at <https://www.mdpi.com/article/10.3390/nano11082133/s1>, Figure S1: BaTi_{0.8}Cu_{0.2}O₃ characterization data: (a) DRX diffractograms, and (b) Raman spectra, (c) XPS spectra corresponding to Cu2p3/2 and O1s transitions, and (d) H₂-TPR profiles.; Figure S2: DRIFT spectra recorded for the BaTi_{0.8}Cu_{0.2}O₃ catalyst during a NO_x storage cycle at (a) 300 °C, (b) 350 °C, (c) 400 °C and (d) 450 °C in 500 ppm NO + 5% O₂ in N₂ atmosphere; Figure S3: XPS of the C1s transition for the BaTi_{0.8}Cu_{0.2}O₃ catalyst after 5 NO_x storage–reduction cycles (BTCuO_2_NSR), followed by 1 h term NO_x adsorption experiment in 500 ppm NO + 5% O₂ in N₂ atmosphere (BTCuO_2_sat) and finally regenerated in 10% H₂/N₂ atmosphere; Figure S4: NO and NO₂ concentration registered for BaTi_{0.8}Cu_{0.2}O₃ catalyst during a TPR experiment in 500 ppm NO + 5% O₂ atmosphere balanced with N₂. (see details in Experimental Section); Figure S5: NO and NO₂ concentration registered for BaTi_{0.8}Cu_{0.2}O₃ catalyst during a TPR experiment in 500 ppm NO₂ + 5% O₂ atmosphere balanced with N₂. (see details in Experimental Section); Table S1: XPS characterization data for BaTi_{0.8}Cu_{0.2}O₃.

Author Contributions: Conceptualization, V.A.-F., J.A.A. and M.-J.I.-G.; methodology, V.A.-F. and J.A.A.; validation, V.A.-F., J.A.A. and M.-J.I.-G.; formal analysis, V.A.-F., M.-S.S.-A. and M.-J.I.-G.; investigation, V.A.-F.; resources, J.A.A. and M.-J.I.-G.; data curation, V.A.-F.; writing—original draft preparation, V.A.-F. and M.-S.S.-A.; writing—review and editing, J.A.A. and M.-J.I.-G.; visualization, M.-S.S.-A.; supervision, J.A.A. and M.-J.I.-G.; project administration, J.A.A. and M.-J.I.-G.; funding acquisition, J.A.A. and M.-J.I.-G. All authors have read and agreed to the published version of the manuscript.

Funding: This research was funded by Generalitat Valenciana (PROMETEO/2018/076 and Spanish Government (PID2019-105542RB-I00) and EU (FEDER Funding).

Conflicts of Interest: The authors declare no conflict of interest.

References

1. Epling, W.S.; Campbell, L.E.; Yezerets, A.; Currier, N.W.; Parks, J.E. Overview of the Fundamental Reactions and Degradation Mechanisms of NO_x Storage/Reduction Catalysts. *Catal. Rev.* **2004**, *46*, 163–245. [[CrossRef](#)]
2. Roy, S.; Baiker, A. NO_x Storage–Reduction Catalysis: From Mechanism and Materials Properties to Storage–Reduction Performance. *Chem. Rev.* **2009**, *109*, 4054–4091. [[CrossRef](#)] [[PubMed](#)]
3. Liu, G.; Gao, P.-X. A review of NO_x storage/reduction catalysts: Mechanism, materials and degradation studies. *Catal. Sci. Technol.* **2011**, *1*, 552–568. [[CrossRef](#)]
4. Pereda-Ayo, B.; González-Velasco, J.R. NO_x Storage and Reduction for Diesel Engine Exhaust Aftertreatment. In *Diesel Engine-Combustion, Emissions and Condition Monitoring*; InTechOpen: London, UK, 2013; p. 266. [[CrossRef](#)]
5. Fridell, E.; Skoglundh, M.; Björnwesterbergab, B.; Johanssonac, S.; Smedlera, G. NO_xStorage in Barium-Containing Catalysts. *J. Catal.* **1999**, *183*, 196–209. [[CrossRef](#)]
6. Broqvist, P.; Panas, I.; Fridell, E.; Persson, H. NO_x Storage on BaO(100) Surface from First Principles: A Two Channel Scenario. *J. Phys. Chem. B* **2001**, *106*, 137–145. [[CrossRef](#)]
7. Anderson, J.A.; Bachiller-Baeza, B.; Fernández-García, M. Role of Pt in Pt/Ba/Al₂O₃ NO_x storage and reduction traps. *Phys. Chem. Chem. Phys.* **2003**, *5*, 4418–4427. [[CrossRef](#)]
8. Liu, Z.; Anderson, J.A. Influence of reductant on the thermal stability of stored NO_x in Pt/Ba/Al₂O₃ NO_x storage and reduction traps. *J. Catal.* **2004**, *224*, 18–27. [[CrossRef](#)]
9. Ayo, B.P.; De La Torre, U.; Marcos, M.P.G.; González-Velasco, J.R. Influence of ceria loading on the NO_x storage and reduction performance of model Pt–Ba/Al₂O₃ NSR catalyst. *Catal. Today* **2015**, *241*, 133–142. [[CrossRef](#)]
10. Ji, Y.; Toops, T.J.; Pihl, J.A.; Crocker, M. NO_x storage and reduction in model lean NO_x trap catalysts studied by in situ DRIFTS. *Appl. Catal. B Environ.* **2009**, *91*, 329–338. [[CrossRef](#)]

11. Lietti, L.; Daturi, M.; Blasin-Aubé, V.; Ghiotti, G.; Prinetto, F.; Forzatti, P. Relevance of the Nitrite Route in the NO_x Adsorption Mechanism over Pt-Ba/Al₂O₃ NO_x Storage Reduction Catalysts Investigated by using Operando FTIR Spectroscopy. *ChemCatChem* **2011**, *4*, 55–58. [[CrossRef](#)]
12. Fridell, E.; Persson, H.; Westerberg, B.; Olsson, L.; Skoglundh, M. The mechanism for NO_x storage. *Catal. Lett.* **2000**, *66*, 71–74. [[CrossRef](#)]
13. Castoldi, L.; Lietti, L.; Righini, L.; Forzatti, P.; Morandi, S.; Ghiotti, G. FTIR and Transient Reactivity Experiments of the Reduction by H₂, CO and HCs of NO_x Stored Over Pt-Ba/Al₂O₃ LNTs. *Top. Catal.* **2013**, *56*, 193–200. [[CrossRef](#)]
14. Lietti, L.; Righini, L.; Castoldi, L.; Artioli, N.; Forzatti, P. Labeled ¹⁵N Study on N₂ and N₂O Formation Over Pt-Ba/Al₂O₃ NSR Catalysts. *Top. Catal.* **2013**, *56*, 7–13. [[CrossRef](#)]
15. Castoldi, L.; Nova, I.; Lietti, L.; Forzatti, P. Study of the effect of Ba loading for catalytic activity of Pt-Ba/Al₂O₃ model catalysts. *Catal. Today* **2004**, *96*, 43–52. [[CrossRef](#)]
16. Shi, C.; Ji, Y.; Graham, U.M.; Jacobs, G.; Crocker, M.; Zhang, Z.; Wang, Y.; Toops, T.J. NO_x storage and reduction properties of model ceria-based lean NO_x trap catalysts. *Appl. Catal. B Environ.* **2012**, *119–120*, 183–196. [[CrossRef](#)]
17. Su, Y.; Amiridis, M.D. In situ FTIR studies of the mechanism of NO_x storage and reduction on Pt/Ba/Al₂O₃ catalysts. *Catal. Today* **2004**, *96*, 31–41. [[CrossRef](#)]
18. Sedlmair, C.; Seshan, K.; Jentys, A.; Lercher, J.A. Elementary steps of NO_x adsorption and surface reaction on a commercial storage-reduction catalyst. *J. Catal.* **2003**, *214*, 308–316. [[CrossRef](#)]
19. Hodjati, S.; Petit, C.; Pitchon, V.; Kiennemann, A. Absorption/desorption of NO_x process on perovskites: Nature and stability of the species formed on BaSnO₃. *Appl. Catal. B Environ.* **2000**, *27*, 117–126. [[CrossRef](#)]
20. Milt, V.; Ulla, M.; Miró, E. NO_x trapping and soot combustion on BaCoO_{3–y} perovskite: LRS and FTIR characterization. *Appl. Catal. B Environ.* **2005**, *57*, 13–21. [[CrossRef](#)]
21. Abrahamsson, B.; Grönbeck, H. NO_x Adsorption on AlTiO₃(001) Perovskite Surfaces. *J. Phys. Chem. C* **2015**, *119*, 18495–18503. [[CrossRef](#)]
22. López-Suárez, F.; Illán-Gómez, M.; Bueno-López, A.; Anderson, J.A. NO_x storage and reduction on a SrTiCuO₃ perovskite catalyst studied by operando DRIFTS. *Appl. Catal. B Environ.* **2011**, *104*, 261–267. [[CrossRef](#)]
23. Albaladejo-Fuentes, V.; E López-Suárez, F.; Sánchez-Adsuar, M.S.; Illán-Gómez, M.J. BaTi_{1–x}Cu_xO₃ perovskites: The effect of copper content in the properties and in the NO_x storage capacity. *Appl. Catal. A Gen.* **2014**, *488*, 189–199. [[CrossRef](#)]
24. Pechini, M.P. Method of Preparing Lead and Alkaline Earth Titanates and Niobates and Coating Method Using the Same to form a Capacitor. U.S. Patent No. 3330697, 11 July 1967.
25. Kareiva, A.; Tautkus, S.; Rapalaviciute, R.; Jørgensen, J.-E.; Lundtoft, B. Sol-gel synthesis and characterization of barium titanate powders. *J. Mater. Sci.* **1999**, *34*, 4853–4857. [[CrossRef](#)]
26. Narendar, Y.; Messing, G.L. Mechanisms of phase separation in gel-based synthesis of multicomponent metal oxides. *Catal. Today* **1997**, *35*, 247–268. [[CrossRef](#)]
27. Hadjiivanov, K.I. Identification of Neutral and Charged NxOy Surface Species by IR Spectroscopy. *Catal. Rev.* **2000**, *42*, 71–144. [[CrossRef](#)]
28. Roedel, E.; Urakawa, A.; Kureti, S.; Baiker, A. On the local sensitivity of different IR techniques: Ba species relevant in NO_x storage-reduction. *Phys. Chem. Chem. Phys.* **2008**, *10*, 6190–6198. [[CrossRef](#)] [[PubMed](#)]
29. Frola, F.; Manzoli, M.; Prinetto, F.; Ghiotti, G.; Castoldi, L.; Lietti, L. Pt-Ba/Al₂O₃ NSR Catalysts at Different Ba Loading: Characterization of Morphological, Structural, and Surface Properties. *J. Phys. Chem. C* **2008**, *112*, 12869–12878. [[CrossRef](#)]
30. Prinetto, F.; Ghiotti, G.; Nova, I.; Lietti, L.; Tronconi, E.; Forzatti, P. FT-IR and TPD Investigation of the NO_x Storage Properties of BaO/Al₂O₃ and Pt-BaO/Al₂O₃ Catalysts. *J. Phys. Chem. B* **2001**, *105*, 12732–12745. [[CrossRef](#)]
31. Wu, N.L.; Tschamber, V.; Limousy, L.; Michelin, L.; Westermann, A.; Azambre, B.; Fehete, I.; Garin, F. Combined Fixed-Bed Reactor and In Situ DRIFTS Tests of NO Adsorption on a NO_x Storage-Reduction System Catalyst. *Chem. Eng. Technol.* **2013**, *37*, 204–212. [[CrossRef](#)]
32. Kim, D.H.; Kwak, J.H.; Szanyi, J.; Burton, S.D.; Peden, C.H. Water-induced bulk Ba(NO₃)₂ formation from NO₂ exposed thermally aged BaO/Al₂O₃. *Appl. Catal. B Environ.* **2007**, *72*, 233–239. [[CrossRef](#)]
33. Briggs, D. Handbook of X-ray Photoelectron Spectroscopy C. D. Wanger, W. M. Riggs, L. E. Davis, J. F. Moulder and G. E. Muilenberg Perkin-Elmer Corp., Physical Electronics Division, Eden Prairie, Minnesota, USA, 1979. 190 pp. \$195. *Surf. Interface Anal.* **1981**, *3*. [[CrossRef](#)]
34. Merino, N.A.; Barbero, B.P.; Eloy, P.; Cadús, L.E. La_{1–x}Ca_xCoO₃ perovskite-type oxides: Identification of the surface oxygen species by XPS. *Appl. Surf. Sci.* **2006**, *253*, 1489–1493. [[CrossRef](#)]
35. Lotnyk, A.; Senz, S.; Hesse, D. Formation of BaTiO₃ thin films from (110) TiO₂ rutile single crystals and BaCO₃ by solid state reactions. *Solid State Ionics* **2006**, *177*, 429–436. [[CrossRef](#)]
36. Leipner, H.S.; Abicht, H.-P.; Hollricher, O.; Gablenz, S. Raman microscopic investigations of BaTiO₃ precursors with core-shell structure. *Anal. Bioanal. Chem.* **2004**, *380*, 157–162. [[CrossRef](#)]
37. Templeton, L.K.; Pask, J.A. Formation of BaTiO₃ from BaCO₃ and TiO₂ in Air and in CO₂. *J. Am. Ceram. Soc.* **1959**, *42*, 212–216. [[CrossRef](#)]
38. Niepce, J.C.; Thomas, G. About the mechanism of the solid-way synthesis of barium metatitanate. industrial consequences. *Solid State Ion.* **1990**, *43*, 69–76. [[CrossRef](#)]
39. Mukhopadhyay, S.M.; Chen, T.C. Surface chemical states of barium titanate: Influence of sample processing. *J. Mater. Res.* **1995**, *10*, 1502–1507. [[CrossRef](#)]

40. Szanyi, J.; Kwak, J.H.; Hanson, J.; Wang, C.; Szailer, T.; Peden, C.H.F. Changing Morphology of BaO/Al₂O₃ during NO₂ Uptake and Release. *J. Phys. Chem. B* **2005**, *109*, 7339–7344. [[CrossRef](#)] [[PubMed](#)]
41. Beauger, A.; Mutin, J.C.; Niepce, J.C. Role and behaviour of orthotitanate Ba₂TiO₄ during the processing of BaTiO₃ based ferroelectric ceramics. *J. Mater. Sci.* **1984**, *19*, 195–201. [[CrossRef](#)]
42. Schneider, W.F. Qualitative Differences in the Adsorption Chemistry of Acidic (CO₂, SO_x) and Amphiphilic (NO_x) Species on the Alkaline Earth Oxides. *J. Phys. Chem. B* **2004**, *108*, 273–282. [[CrossRef](#)]
43. Vovk, E.I.; Turksoy, A.; Bukhtiyarov, V.I.; Ozensoy, E. Interactive Surface Chemistry of CO₂ and NO₂ on Metal Oxide Surfaces: Competition for Catalytic Adsorption Sites and Reactivity. *J. Phys. Chem. C* **2013**, *117*, 7713–7720. [[CrossRef](#)]
44. Kim, D.H.; Chin, Y.-H.; Kwak, J.H.; Szanyi, J.; Peden, C.H. Changes in Ba Phases in BaO/Al₂O₃ upon Thermal Aging and H₂O Treatment. *Catal. Lett.* **2005**, *105*, 259–268. [[CrossRef](#)]
45. López, M.D.C.B.; Fourlaris, G.; Rand, B.; Riley, F.L. Characterization of Barium Titanate Powders: Barium Carbonate Identification. *J. Am. Ceram. Soc.* **1999**, *82*, 1777–1786. [[CrossRef](#)]
46. Xian, H.; Zhang, X.; Li, X.; Zou, H.; Meng, M.; Zou, Z.; Guo, L.; Tsubaki, N. Raman microscopic investigations of BaTiO₃ precursors with core-shell structure. *Catal. Today* **2010**, *158*, 215–219. [[CrossRef](#)]
47. Emmez, E.; Vovk, E.I.; Bukhtiyarov, V.I.; Ozensoy, E. Direct Evidence for the Instability and Deactivation of Mixed-Oxide Systems: Influence of Surface Segregation and Subsurface Diffusion. *J. Phys. Chem. C* **2011**, *115*, 22438–22443. [[CrossRef](#)]
48. Piacentini, M.; Maciejewski, M.; Baiker, A. Pt-Ba/alumina NO_x storage-reduction catalysts: Effect of Ba-loading on build-up, stability and reactivity of Ba-containing phases. *Appl. Catal. B Environ.* **2005**, *59*, 187–195. [[CrossRef](#)]